JOURNAL OF MATERIALS SCIENCE 16 (1981) 2269–2280

The solidification and mechanical properties of chill-cast Al–Al_3Ni and Al–Al_2Cu eutectic alloys

F. S. J. JABCZYNSKI,* B. CANTOR†
Department of Engineering and Applied Sciences, University of Sussex, Falmer, Brighton, Sussex, UK

This paper describes the effect of chill-casting on the solidification behaviour and mechanical properties of the Al–Al_3Ni and Al–Al_2Cu eutectic alloys. Cellular microstructures were obtained by casting the eutectic alloys into preheated split-steel moulds mounted on either a water-cooled or plain copper chill, to promote growth along the length of the ingot and not radially from the mould wall. This produced the required cellular microstructure with good alignment of Al_3Ni fibres or Al_2Cu lamellae within the cells, with an interfibre/interlamellar spacing of $\sim 1\ \mu m$. The experimental solidification results showed an increase in solidification rate with increasing distance from the chill associated with a decrease in interfibre/interlamellar spacing along the length of the solidifying ingot. There were no significant variations in the room-temperature tensile properties of the two chill-cast aluminium based eutectic alloys for the various casting conditions. Variations in solidification rate along the ingots for the different chill-casting conditions were not sufficient to affect the stress–strain behaviour of the chill-cast alloys. The room-temperature tensile behaviour of the chill-cast Al–Al_3Ni eutectic alloy was very similar to, and that of the Al–Al_2Cu eutectic alloy significantly different from, those obtained by Lawson and Kerr. The ultimate tensile strengths of the chill-cast eutectic alloys were not as high as those of the corresponding unidirectionally-solidified eutectic alloys prepared at a slow and constant solidification rate although the reasons for this were different for the two alloys. The ultimate tensile strength of the chill-cast Al–Al_3Ni eutectic alloy was found to be in reasonable agreement with that expected from the rule of mixtures for discontinuous fibre reinforcement.

1. Introduction

To obtain a regularly aligned eutectic composite special care has to be taken concerning the purity of the melt, temperature gradient and solidification rate during the unidirectional solidification process. Other microstructures can result if these conditions are not attained. A colony microstructure is obtained if the value of the temperature gradient/solidification rate ratio is below the critical value (which varies with different eutectic alloys) required to produce a plane solidification front in unidirectionally-solidifying eutectic alloys. This colony microstructure is cellular with poor alignment in the cell walls. However, the majority of the fibres or lamellae within the cells (or colonies) are well aligned. This phenomenon was discovered in 1927 by Hargreaves [1] but, despite this early work, it was not until the late 1950's that research work on colonies was reconsidered. It is now recognized that colonies are the result of solidifi-

*Present address: Department of Physical Metallurgy and Science of Materials, University of Birmingham, North Campus, Elms Road, PO Box 363, Birmingham, UK.
†Present address: Department of Physical Metallurgy and Science of Materials, University of Oxford, Oxford, UK.

0022–2461/81/082269–12$03.20/0

cation with a non-planar liquid–solid interface, analogous to the formation of cells in single phase unidirectional solidification, and are caused by the inability of impurities to diffuse away from the interface rapidly enough [2].

The interest in unidirectionally-solidified eutectic alloys has arisen from their potential value as *in situ* reinforced composites. To date, over 150 alloys have been aligned by unidirectional solidification, as reported by Hogan *et al.* [3], and in many cases the resulting mechanical properties have also been investigated. Many authors for instance, have studied the room-temperature tensile behaviour of unidirectionally-solidified Al–Al_3Ni and Al–Al_2Cu eutectic alloys [4–7]. However, very little work has been performed on the partially-aligned or colony microstructure which results at higher solidification rates.

The aim of the work described in this paper was to study both the solidification behaviour and room-temperature tensile properties of chill-cast Al–Al_3Ni and Al–Al_2Cu eutectic alloys. Lawson and Kerr [8], have performed studies on the colony microstructures for the above two eutectic alloys using specimens produced with a vertical type crystal grower, which enabled a constant solidification rate to be maintained. However, chill-casting with a preheated mould presents an easier, inexpensive way of producing partially-aligned eutectic alloys with a colony microstructure.

2. Experimental procedure

Master alloys of the eutectics Al–Al_3Ni and Al–Al_2Cu were prepared from aluminium of 99.9% purity and nickel and copper of 99.99% purity, at the nominal compositions of 6.1 wt% Ni and 33.2 wt% Cu, respectively. Alloying was carried out by melting the constituents together in an alumina crucible under flowing argon. After solidification, each master alloy was sectioned for microscopic examination to ensure homogeneity.

The eutectic alloys were remelted under flowing argon to prevent oxidation prior to being chill-cast. The chill-casting operation was performed by pouring the eutectic melt into a preheated mild steel split-mould placed on either a large copper block (LC) or a water-cooled copper chill (WC). To determine the solidification rates and temperature gradients during chill-casting four chromel–alumel thermocouples were placed at 20 mm intervals along the length of the solidifying ingot. The four thermocouples were connected to a four-pointer potentiometric-type pen recorder (Cambridge Instrument Company Ltd). The pen recorder made a measurement every 3 sec, with a resulting 12 sec interval between successive measurements on a particular thermocouple input. This enabled plots of temperature against solidification time to be obtained conveniently for each of the thermocouples positions during a casting.

Chill-cast ingots of both eutectics under the various chill-casting conditions, were sectioned at 10 mm intervals along the lengths of the ingots to enable the microstructures to be examined. The sections were mechanically polished and etched using Keller's reagent (95% H_2O, 3% concentrated HNO_3, 1.5% concentrated HCl and 0.5% HF). Photographs of the various sections were taken using a Cambridge Mk IIA Stereoscan electron microscope. A line-intercept method was employed to measure the interfibre or interlamellar spacing of the chill-cast eutectics within the colonies.

Tensile specimens were machined from the chill-cast eutectic specimens to a gauge diameter of 3 mm and gauge length of 50 mm. These specimens were then tested using an Instron testing machine with a 4.45 kN load cell and a cross-head speed of 2.1×10^{-5} msec^{-1}. An Instron 50.8 mm 10% strain gauge extensometer was attached to each specimen to measure extensions. All the tensile tests were carried out at room temperature. The resulting fracture surfaces of the tensile specimens were examined in the Stereoscan electron microscope.

3. Results and discussion

3.1. Solidification behaviour

Fig. 1a and b, show typical variations of temperature against time for the Al–Al_3Ni (800WC)* and the Al–Al_2Cu (700LC) chill-cast alloys, respectively. Assuming the solid–liquid interface was at the eutectic temperature T_e, it was possible from these graphs to determine the solidification rate (R), liquid and solid temperature gradients at the solid–liquid interface (G_L and G_S) and the liquid temperature gradient/solidification rate ratio (G_L/R), in each case as a function of the distance

*This notation refers to the chill-casting conditions and is used throughout this paper. The number refers to the mould temperature in degrees centigrade and the following two letters, WC and LC, to the type of chill, i.e. water-cooled or solid copper, respectively.

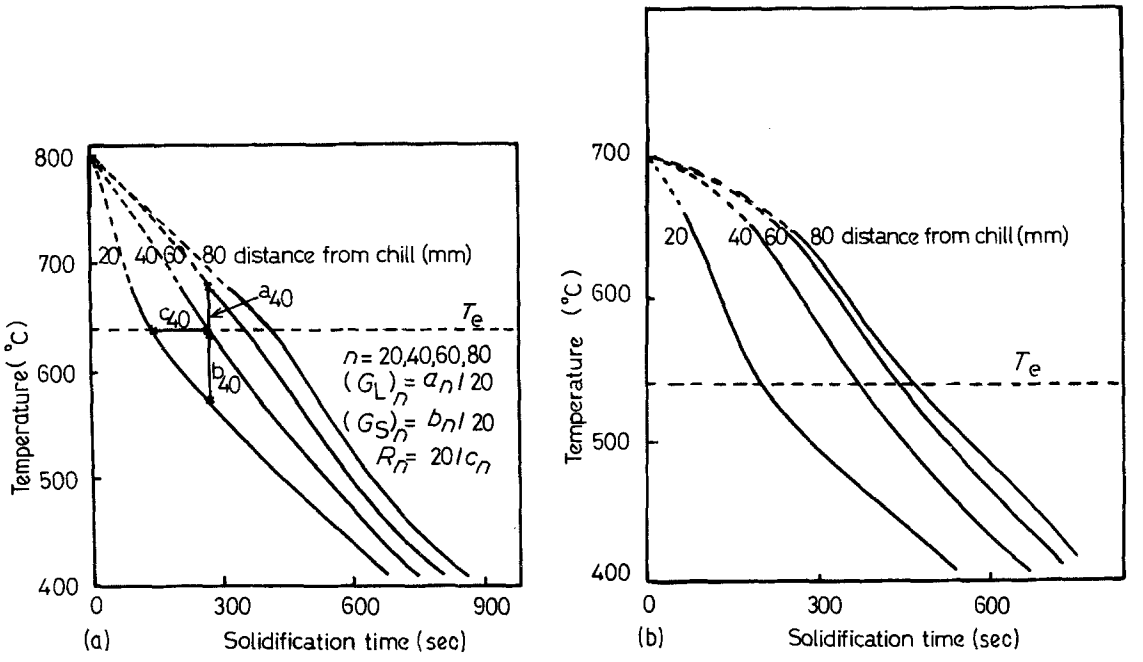

Figure 1 (a) Temperature against solidification time plots for the four thermocouples placed at 20 mm intervals along the length of the mould, for the solidifying Al–Al_3Ni chill-cast (800 WC) eutectic alloy and (b) temperature against solidifying time plots for the four thermocouples placed at 20 mm intervals along the length of the mould, for the solidifying Al–Al_2Cu chill-cast (700 LC) eutectic alloy.

from the chill. The results are shown in Fig. 2a to d for the four combinations of eutectic alloy, superheat and chill block which were used (AN700WC, AN800LC, AN800WC and AN700LC). As can be seen, in all cases R increased while G_L, G_S and G_L/R decreased continuously during solidification. To explain this solidification behaviour, it is necessary to consider the heat flow during solidification and the analytical solution relating to it. As the mould in the simple chill-casting system is preheated to a temperature above the eutectic temperature assume that solidification is unidirectional from the chill, i.e. there is no solidification from the mould walls. Now, consider the solidification of a pure metal. For many types of ingot-casting processes, the thermal resistance of the metal, the chill–metal interface, and the chill surroundings must be considered for a complete solution. Exact analytic solutions are available for some limiting cases of engineering interest. Consider the case when heat flow is one-dimensional, the chill–metal interface resistance is neglible, there is no temperature gradient in the liquid and the chill is either held at constant temperature [as by water-cooling (WC)] or is very thick (LC). Temperature distributions for these cases are shown in Fig. 3.

Firstly, consider the case of the water-cooled chill. The solution to this problem must conform with the partial differential equation

$$\frac{\delta T}{\delta t} = \alpha \cdot \frac{\delta^2 T}{\delta x^2} ; \tag{1}$$

$$\alpha = k/\rho C_p , \tag{2}$$

where α, k, ρ and C_p are thermal diffusivity, thermal conductivity, density and specific heat of the metal, respectively, t is time, T is the temperature and x is the distance from the chill. The boundary conditions at the chill–metal interface are $x = 0$, $T = T_0$, and at the liquid–solid interface are $x = X$ and $T = T_m$, and

$$k \cdot \left(\frac{\delta T}{\delta x}\right)_{x=X} = H_f \cdot \rho \cdot \frac{dx}{dt} , \tag{3}$$

where H_f is the latent heat of fusion of metal, T_m is the melting point of the metal and T_0 is the initial temperature of the chill, i.e. the rate of evolution of latent heat of fusion equals the heat flux into the solid at the interface. The solution given by Carslaw and Jaeger [9] is

$$X = 2 \cdot \beta \cdot (\alpha t)^{1/2} , \tag{4}$$

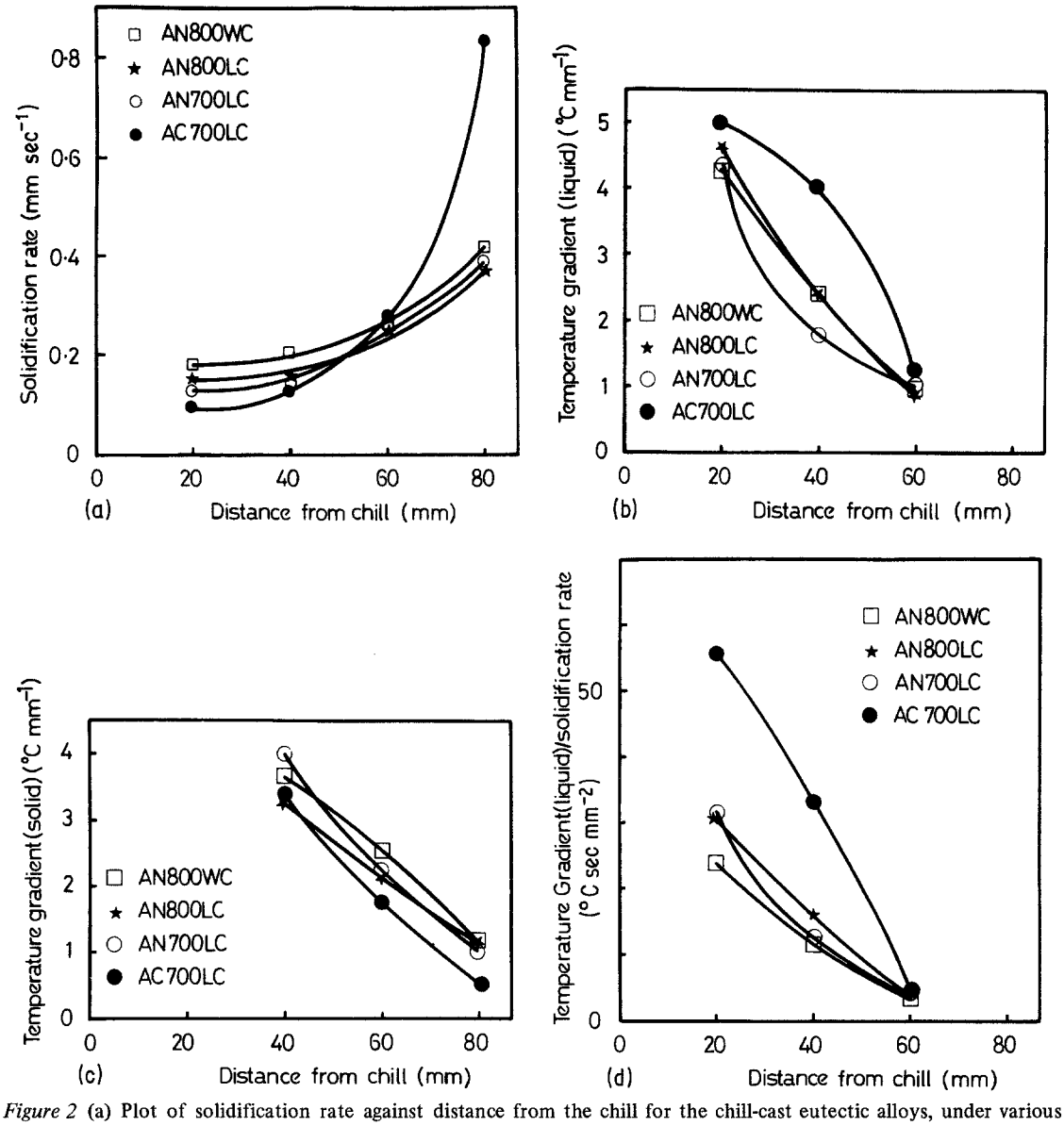

Figure 2 (a) Plot of solidification rate against distance from the chill for the chill-cast eutectic alloys, under various chill-casting condiditons, (b) plot of temperature gradient within the liquid at the solid/liquid interface against distance from the chill for the chill-cast eutectic alloys. under various chill-casting conditions, (c) plot of temperature gradient within the solid at the solid/liquid interface against distance from the chill for the chill-cast eutectic alloys, under various chill-casting conditions and (d) plot of temperature gradient within the liquid/solidification rate ratio against distance from the chill for the chill-cast eutectic alloys, under various chill-casting conditions.

i.e. of the form

$$X = a \cdot t^{1/2}, \tag{5}$$

where, a is a constant and β is determined from

$$\beta \cdot e^{\beta^2} \cdot \operatorname{erf} \beta = \frac{(T_m - T_0) \cdot C_p}{H_f \cdot \pi^{1/2}}, \tag{6}$$

where erf is the error function. The temperature distribution in the solidifying metal is given by

$$\frac{T - T_0}{T_0' - T_0} = \operatorname{erf} \frac{x}{2(\alpha \cdot t)^{1/2}}, \tag{7}$$

where T_0' is an integration constant. The solution when the chill is not water cooled, but is semi-infinite, is a little more complicated. However, like the water-cooled case the amount solidified is parabolic with time [9, 10]. In previous work [11], the theoretical results for the solidification of pure iron against different chills were found to agree with the experimental curves except that the latter were displaced on the time axis. Several investigators e.g. [12] have obtained experimental

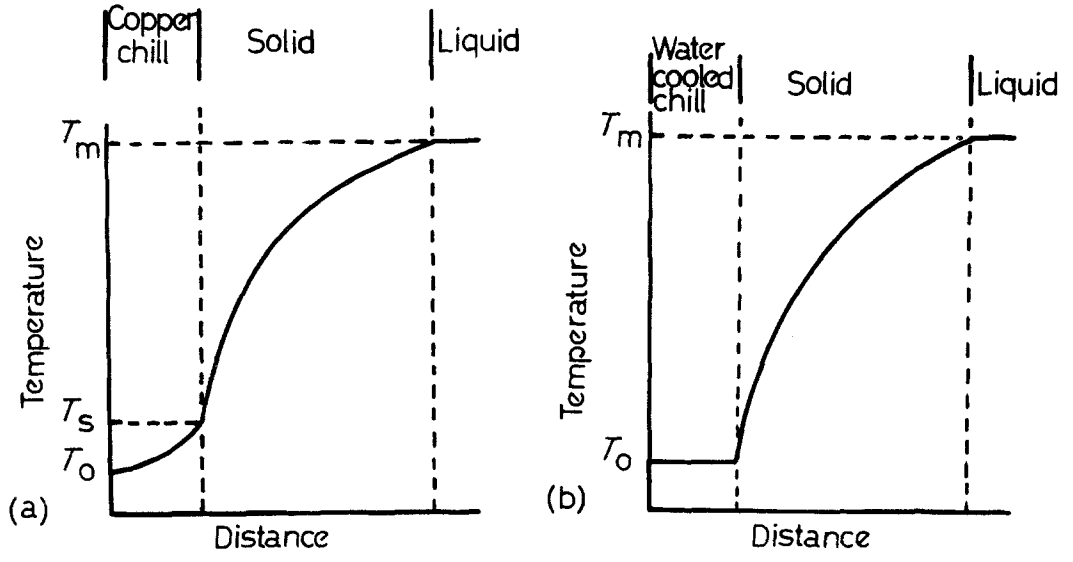

Figure 3 Temperature profiles for solidification against a flat chill when: (a) resistance of solidifying metal is controlling and, (b) combined resistance of metal and chill are controlling.

results for steel solidified against cast iron mould walls which are of the form

$$x = a(t)^{1/2} - b, \tag{8}$$

where a and b are constants. The apparent delay in the beginning of solidification that is found experimentally results from two causes. Firstly, convection during and just after pouring results in rapid removal of superheat from the liquid, thus slowing the start of solidification and its initial rate. The second effect is a finite chill–metal inferface resistance to heat transfer. In this case, the solidification rate is finite at zero time; solidification is interface controlled and so proceeds at a slower rate than in the absence of this resistance. Initially, the amount solidified increases linearly with time, later as the thermal resistance of the solidified metal becomes large compared with the chill–metal interface resistance, the amount solidified increases with the square root of time as in Equation 4.

The preceding equations have been developed for a pure metal; with alloys, solidification occurs over a range of temperatures rather than at a discrete melting point, T_m. However, in the case of eutectic alloys there is a discrete melting point, T_e, and thus the solidification profile would be

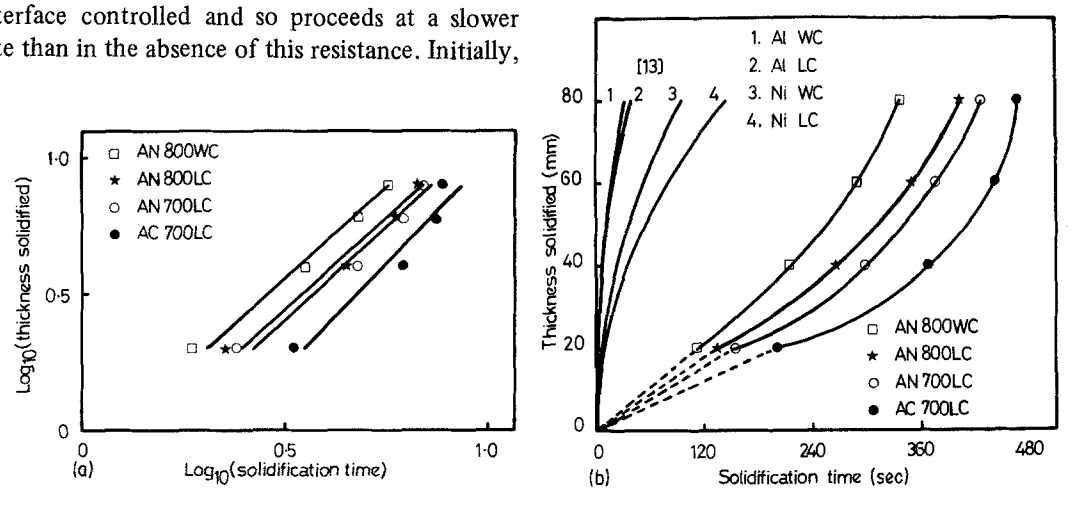

Figure 4 (a) Plot of $\log_{10}$ (thickness solidified) against $\log_{10}$ (solidification time) for the chill-cast eutectic alloys, under various chill-casting conditions and (b) plot of thickness solidified against solidification time for the chill-cast eutectic alloys, under various chill-casting conditions.

similar to that of pure metals. The solidification results obtained using the simple chill-casting system for the two eutectics, Al–Al_3Ni and Al–Al_2Cu seen in Fig. 2a are replotted in Fig. 4a and b. Fig. 4a shows the variation of $\log_{10}$ (thickness solidified) as a function of $\log_{10}$ (solidification time), and Fig. 4b shows the same curves replotted as distance solidified against time using the values of the gradients and intercepts on Fig. 4a, i.e. assuming $x = t^n - c$, $\log_{10} x = n \log_{10} t - \log_{10} c$). Also included are four calculated curves based on Equation 4 for pure aluminium and nickel [13]. From Fig. 4a and b, it can be seen that the four experimental curves are similar is shape. The initial solidification is slow which is probably caused, as mentioned previously, by removal of superheat from the liquid and by chill–metal resistance to heat transfer. Later, as the thermal resistance of the solidifying metal becomes large compared with that of the chill–metal interface, the amount solidified is proportional to t^n where n is 1.34 ± 0.21 for the Al–Al_3Ni eutectic and 1.54 ± 0.29 for the Al–Al_2Cu eutectic. This is different to that expected from the analysis above, and therefore different to that calculated for the chill-cast pure metals where the amount solidified is proportional to $t^{1/2}$.

This difference can be explained as follows. In the theoretical calculations for the pure metals it was assumed that there was no temperature gradient in the liquid which (Equation 1) led to a solidification equation of the form of Equation 5. However, from Fig. 2b, which shows the temperature gradient in the liquid as a function of distance from the chill and Fig. 1a and b it can be seen that there is a decreasing temperature gradient in the liquid at the solid/liquid interface along the length of the solidifying ingot. During freezing in commercially-cast ingots (~ 2500 kg) from chills using insulated moulds, the temperature gradient in the liquid ahead of the solid–liquid interface is found to be undetectably small, as reported by Doherty and Melford [14]. The large size of the ingots enabled the superheat in the liquid to be lost rapidly due to the convection currents present. However, in the case of the laboratory size, chill-cast ingots ($\sim 4 \times 10^{-2}$ kg) the superheat is lost more slowly because less convection occurs. By comparing Fig. 2b and c, it can be seen that the temperature gradient in the liquid at the solid/liquid interface is decreasing faster than the corresponding temperature gradient in the solid. Rewriting Equation 3, assuming that there is a temperature gradient in the liquid, leads to the following equation

$$k_s \left(\frac{\delta T}{\delta x}\right)_{s_{x=X}} - k_l \left(\frac{\delta T}{\delta x}\right)_{l_{x=X}} = \rho_s \cdot H_{f_s} \cdot \frac{\delta X}{\delta t}, \quad (9)$$

where the subscripts s and l represent the solid and liquid, respectively. From Equation 9, it can be seen that the result of a decreasing temperature gradient in the liquid at a greater rate than in the solid, at the solid/liquid interface, results in an increasing solidification rate with increasing distance from the chill.

3.2. Microstructure

The Al–Al_3Ni eutectic alloy has a fibrous microstructure, as can be seen from Fig. 5, which shows typical transverse and longitudinal sections of a chill-cast ingot (800WC). In contrast, the Al–Al_2Cu (700LC) eutectic alloy has a lamellar microstructure as can be seen in Fig. 6, which shows similar sections to the above. From these micrographs, the cellular nature of the eutectics produced using the chill-casting set-up is also apparent. The cell diameter was found to vary with the solidification rate along the length of the ingots for both the eutectic alloys. From measurements made on transverse sections within the region 0 to 30 mm from the chill, the cells were circular in cross-section with a cell diameter of approximately 50 μm. Between 30 and 80 mm, the cross-sections contained a mixture of circular cells with a diameter of approximately 50 μm and oval-shaped cells with diameters of approximately 140 μm × 50 μm.

The interfibre and interlamellar spacings for the Al–Al_3Ni and Al–Al_2Cu eutectics, respectively, were measured at 10 mm intervals (at the centres of the cells) along the length of the ingots for the various chill-casting conditions. These measurements are illustrated in Fig. 7a and b. Along with these experimentally determined values, interfibre and interlamellar spacings were calculated from the previously determined relationship between interfibre/lamellar spacing and solidification rate as found by Livingstone *et al.* [15]

$$\lambda = AR^{1/2}, \quad (10)$$

where λ is the interfibre or interlamellar spacing and R is the solidification rate [15]. A is a con-

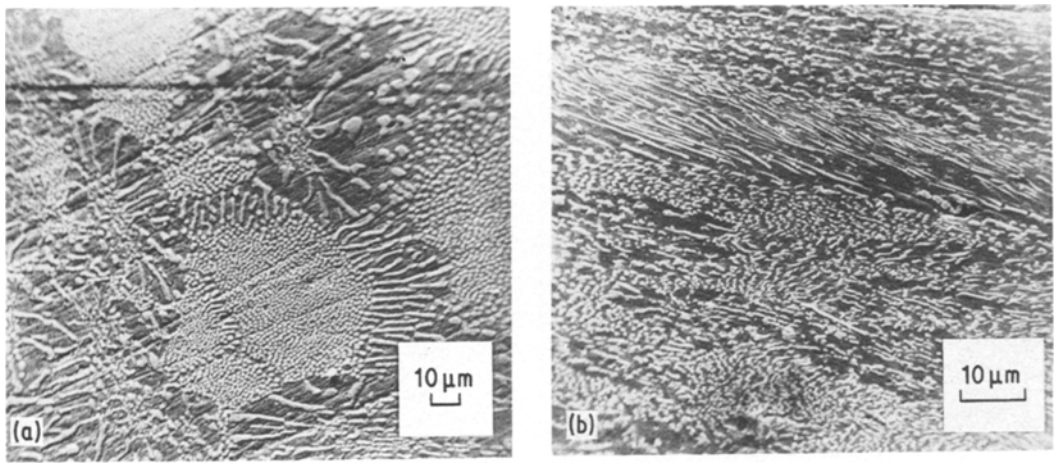

Figure 5 SEM (45° tilt) micrographs of chill-cast Al–Al_3Ni eutectic alloy (800 WC) (a) transverse section, 50 mm from chill, and (b) longitudinal section, 20 mm from chill.

stant with a value of $8 \times 10^{-17} m^{1/2} sec^{1/2}$ for Al–Al_3Ni and Al–Al_2Cu. These calculated spacings are also plotted in Fig. 7a and b.

From the graphs of interfibre and interlamellar spacing against distance from the chill, it can be seen that the spacings tend to decrease along the length of the chill-cast ingots. This is consistent with the increasing solidification rate found from the temperature measurements made during solidification, i.e. a decreasing interfibre/lamellar spacing means an increasing solidification rate. However, the spacings tended to be higher than would be expected from the equation relating spacing with solidification rate (Equation 10). The discrepancy could be due, primarily, to the effect of sectioning through a cellular microstructure which would tend to result in an oversize spacing. Secondly, the larger spacings suggest that the microstructure may have undergone some post-solidification coarsening behind the solid–liquid interface. As argued in the last section, the chill-casting thermal gradients are steep compared to a conventional ingot casting, however, the gradients are very shallow compared to the unidirectional solidification experiments which were used to derive values of A for Equation 10. Thus a greater amount of time is available at high temperature behind the solid–liquid interface for the microstructure to coarsen and the interfibre/lamellar spacing to increase.

3.3. Mechanical properties

The room-temperature tensile data for the chill-cast Al–Al_3Ni and Al–Al_2Cu eutectic alloys are

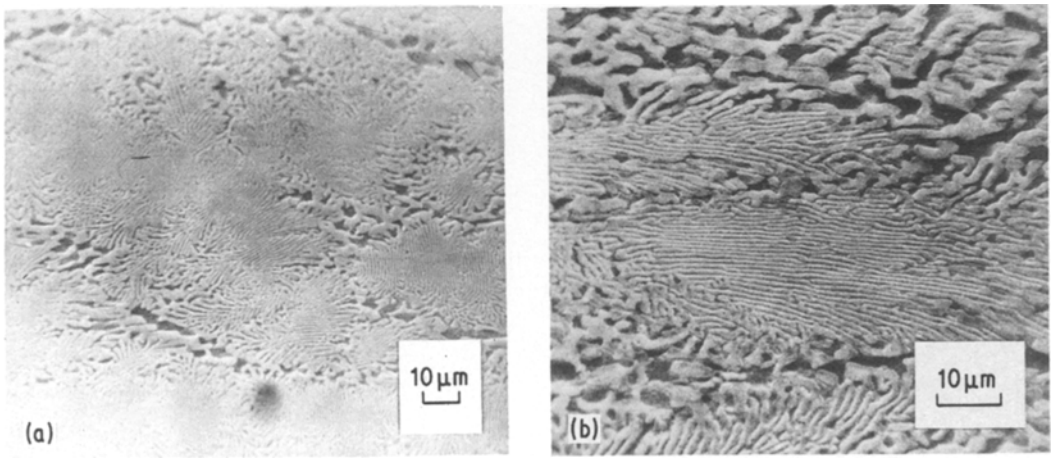

Figure 6 SEM (45° tilt) micrographs of chill-cast Al–Al_2Cu eutectic alloy (700 LC) (a) transverse and (b) longitudinal sections 50 mm from chill.

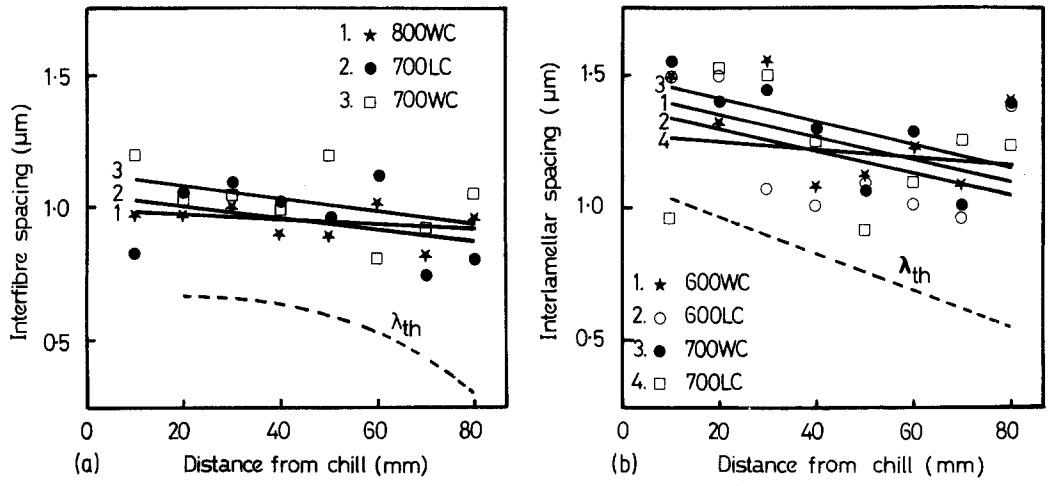

Figure 7 (a) Plot of interfibre spacing against distance from chill for the chill-cast Al–Al_3Ni eutectic alloy under various chill-casting conditions and (b) plot of interlamellar spacing against distance from chill for the chill-cast Al–Al_2Cu eutectic alloy, under various chill-casting conditions.

summarized in Table I. It is apparent that the variation of chill-casting conditions led to no significant change in the ultimate tensile strength; 0.1 and 0.2% offset yield strength and fracture strain for either eutectic. This was in agreement with the results for the solidification behaviour and microstructure. The variations in solidification rate and interfibre/lamellar spacing between the different chill-casting conditions and along the length of the ingots was not sufficient to affect the stress–strain behaviour. The testing procedure was not sensitive enough to determine accurately the elastic limit since the onset of yielding was gradual. Because of this curvature in the initial portion of the stress–strain curve, the determination of the elastic modulus was also difficult and could not be reproduced. Typical stress–strain behaviours for the two alloys under the different chill-casting conditions are shown in Fig. 8a and b, together with comparison curves for the cellular microstructures obtained by Lawson and Kerr [8] using a solidification rate of 4×10^{-4} msec^{-1} and unidirectional solidified data obtained by Cantor *et al.* [7] with a solidification rate of $\sim 3 \times 10^{-5}$ msec^{-1}. The solidification rate of the chill-cast ingots varied from ~ 2 to 4×10^{-4} msec^{-1} along their length (Fig. 2a).

The room-temperature tensile properties of the chill-cast Al–Al_3Ni eutectic produced using the simple chill-casting system were very similar to those obtained by Lawson and Kerr [8]. This is despite the variable solidification rate along the ingots, compared to Lawson and Kerr's steady-state conditions obtained with a more complicated although more controlled solidification set-up. In both cases, the deformation behaviour was characterized by a high and relatively constant work-hardening rate in the initial stages of plastic

TABLE I Mechanical properties of chill-cast Al–Al_3Ni and Al–Al_2Cu eutectic alloys. Each value is the mean of 4 to 5 individual specimens

Alloy	Chill-casting conditions	UTS (MPa)	0.2% offset yield stress (MPa)	0.1% offset yield stress (MPa)	Fracture strain (%)
Al–Al_3Ni	700 WC	214 ± 6	216 ± 5	198 ± 15	3.2 ± 0.1
	700 LC	207 ± 9	–	–	2.8 ± 0.3
	800 WC	219 ± 2	217 ± 1	193 ± 14	3.1 ± 0.5
	800 LC	220 ± 3	220 ± 2	202 ± 8	3.3 ± 0.5
Al–Al_2Cu	600 WC	208 ± 29	–	–	–
	600 LC	202 ± 31	–	–	0.31 ± 0.08
	700 WC	215 ± 19	178 ± 16	136 ± 12	0.30 ± 0.10
	700 LC	224 ± 6	170 ± 28	129 ± 20	0.42 ± 0.03

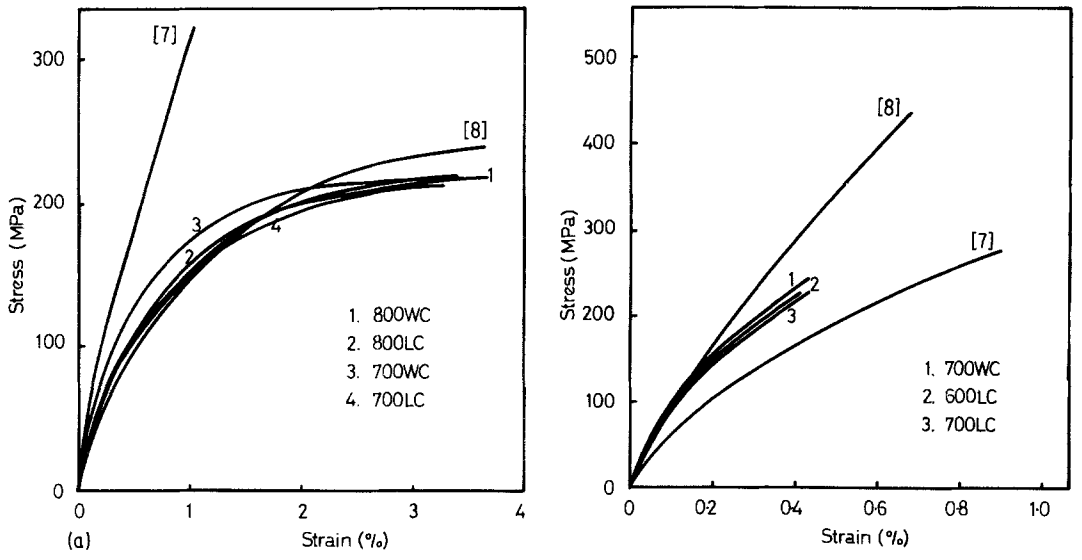

Figure 8 (a) Stress–strain curves for the chill-cast Al–Al_3Ni eutectic alloy with different combinations of mould temperature and chills. Lawson and Kerr's [8] data for the cellular eutectic unidirectionally-solidified at 4×10^{-4} msec^{-1} and Cantor *et al.*'s [7] data for fully aligned eutectic solidified at 3×10^{-5} msec^{-1} are also shown and (b) stress–strain curves for the chill-cast Al–Al_2Cu eutectic alloy with different combinations of mould temperature and chills. Lawson and Kerr's [8] data for the cellular unidirectionally-solidified eutectic at 4×10^{-4} msec^{-1} and Cantor *et al.*'s [7] data for fully aligned eutectic solidified at 3×10^{-5} msec^{-1} are also shown.

deformation followed by a region of continuously decreasing work-hardening up to fracture. The ultimate tensile strength was not as high as that obtained with unidirectionally-solidified eutectic alloy ~ 294 MPa [7], however, the fracture strain was higher, ~ 3 to 4% for the chill-cast Al–Al_3Ni eutectic compared with approximately 1% for the unidirectionally-solidified eutectic. Because of the similar deformation and fracture behaviour within the cells, this suggests that the Al_3Ni fibres provide only an ineffective reinforcement in the colony walls and therefore allow considerable plastic flow in these regions.

From Fig. 8b, it can be seen that both the present work and that of Lawson and Kerr [8] for the Al–Al_2Cu eutectic alloy show a larger work-hardening effect compared to that of Cantor *et al.* [7] for the unidirectionally-solidified alloy. Lawson and Kerr suggest that this large work-hardening was not caused by dislocation pile-up [16] alone as they found the dislocation density was low. Along with other workers [16], they suggest that the different Poisson's ratios of the two phases may produce transverse stresses which constrain a portion of the matrix beyond its usual yield point. Since the transverse stresses would be greatest adjacent to the reinforcing phase, they expected the volume fraction of the constrained matrix to be nearly proportional to the interphase interfacial areas, which they found to be consistent with their observations that the work-hardening rates increase with solidification rate.

As the solidification rates in the present work (~ 2 to 4×10^{-4} msec^{-1}) and that of Lawson and Kerr (4×10^{-4} msec^{-1}) were greater than that used by Cantor *et al.* (3×10^{-5} msec^{-1}) a greater work-hardening effect would be expected as the interlamellar spacings were smaller ($\lambda = AR^{-1/2}$) resulting in a greater volume fraction of the matrix being constrained.

However, the misalignment due to a cellular microstructure opposes the constraint effect. A misaligned region of a composite ceases to make a significant contribution to composite strength when the resolved shear results in matrix flow, as was found with the Al–Al_3Ni chill-cast eutectic. Unlike the Al–Al_3Ni chill-cast eutectic and stress–strain curves for the chill-cast Al–Al_2Cu eutectic show approximately 50% less plastic deformation than the stress–strain curves obtained by either Cantor *et al.* or Lawson and Kerr for the unidirectionally-solidified eutectic. The lower ultimate tensile strengths and fracture strains are therefore not caused by any difference in deformation behaviour (as found for Al–Al_3Ni) but result from premature fracture. This implies that for the chill-cast Al–Al_2Cu eutectic there was no easy flow within the colony walls. Because of the

greater volume fraction of the reinforcing phase (~ 40 vol %) in the Al–Al_2Cu eutectic compared to the Al–Al_3Ni eutectic (~ 10 vol %), large coarse Al_2Cu particles were obtained within the colony walls after chill-casting. Premature failure of these coarse Al_2Cu particles would lead to a premature failure of the eutectic as a whole and a lower ultimate tensile strength and fracture strain. Even though the Al–Al_2Cu eutectic of Lawson and Kerr [8] had a colony microstructure it was probably more like the unidirectionally-solidified eutectic with a smaller interlamellar spacing (and hence a greater constrained matrix effect) and without the coarse Al_2Cu in the colony walls because of a more controlled solidification process. Unfortunately, it was not possible to compare colony sizes as Lawson and Kerr do not give the relevant data.

Failure of the chill-cast Al–Al_3Ni eutectic specimens was not accompanied by extensive shattering of the specimen at the fracture surface, but instead fracture occurred by slow propagation of a single crack. The crack path was not straight across the specimen but was zig-zag in nature. Macroscopically, the fracture surface was found to be at approximately 45° to the tensile axis similar to the fracture of the unidirectionally-solidified eutectic alloy [7]. Fig. 9 shows the microscopic deformation from which the alpha-aluminium matrix was found to fail in a ductile manner after fibre failure at the crack tip, as evident by the dimpled fracture surface. This is again similar to the unidirectionally-solidified eutectic [7]. Fracture of chill-cast Al–Al_2Cu was in all cases sudden and catastrophic. Macroscopically, the fracture surface was at ~ 90° to the tensile axis. Microscopic analysis showed that the alpha-aluminium phase failed in a ductile manner during crack propagation, as shown in Fig. 10. The fracture at the centre of the colonies is similar to that found with the unidirectionally-solidified eutectic, as can be seen in Fig. 10 [7].

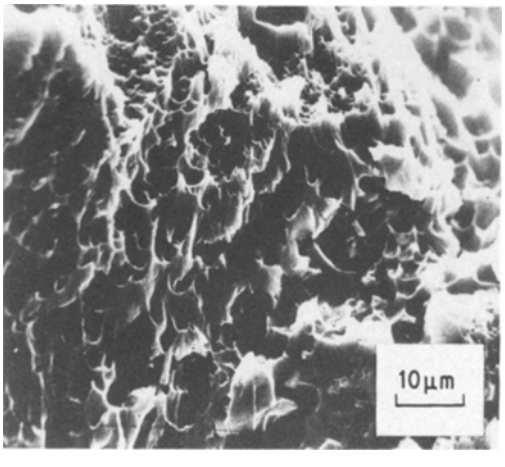

Figure 9 SEM photograph of chill-cast Al–Al_3Ni eutectic alloy (800 WC) fracture surface.

The rule of mixtures for discontinuous fibres can be applied to the chill-cast Al–Al_3Ni eutectic as follows. The law of mixtures, for the ultimate tensile strength for a composite with all the reinforcing fibres in the direction of the tensile axis, is given by [17]

$$\sigma_{ult} = \sigma_f \cdot V_f + \sigma'_m \cdot V_m, \qquad (11)$$

where V_f and V_m are the volume fractions of fibres and matrix, respectively, $V_f > V_{min}$ (i.e. greater than the minimum volume fraction of fibres required for reinforement), σ_f is the ultimate tensile strength of the fibres and σ'_m is the stress borne by the matrix when the strain of the composite is such that the fibres are strained to their ultimate tensile strength. The validity of Equation 11 has been established for unidirectionally-solidified Al–Al_3Ni eutectic alloy [4]. For discontinuous fibres, the rule of mixtures is modified so that [17]

$$\sigma_{ult} = \sigma_f \cdot \left(1 - \frac{l_c}{2l}\right) \cdot V_f + \sigma'_m \cdot V_m \qquad (12)$$

where $l_c/2 = \sigma_f d/4\tau$ is the critical transfer length for reinforcement, d and l are the fibre diameter and length, respectively, and τ is the shear strength of the fibre/matrix interface.

From the work of Hertzberg *et al.* [4], $\sigma_{Al_3Ni} = 2765$ MPa, $V_{Al_3Ni} = 0.11$ and $V_{AL} = 0.89$. From Table I, the mean fracture strain for the chill-cast Al–Al_3Ni eutectic alloy (800WC), was found to 3.14%. The stress–strain curve for chill-cast aluminium using the same casting set-up is shown in Fig. 11. From this the stress borne by the matrix (assuming the matrix is effectively pure aluminium) at 3.14% is 44.1 MPa. Kelly and Tyson [18], have shown that the shear strength at the fibre/matrix interface depends on the strain and measured values of the critical transfer length. They indicate that for work-hardening matrices, the shear strength is equal to the ultimate shear strength of the matrix. Assuming again that the matrix is effectively pure aluminium, the experimentally determined mean ultimate tensile strength of chill-cast aluminium was found to be

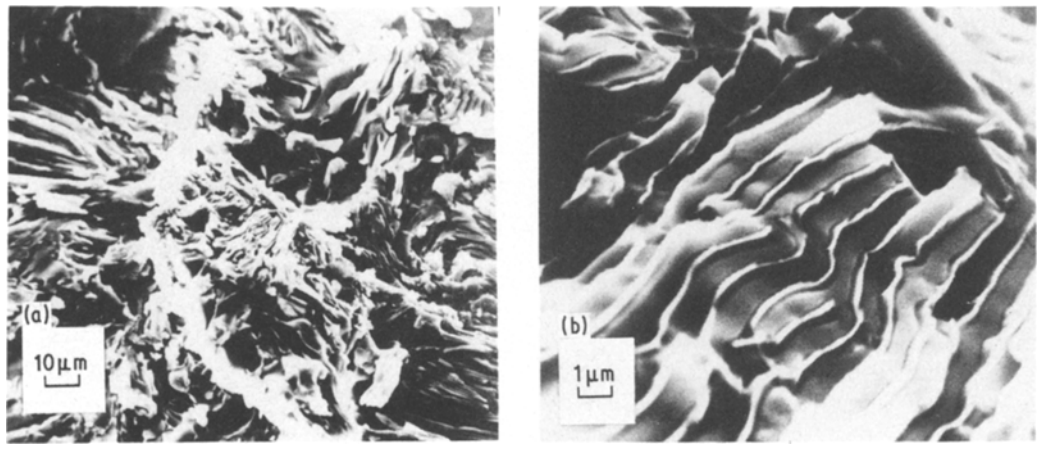

Figure 10. SEM photographs of chill-cast Al–Al_2Cu eutectic alloy (700 LC) fracture surface at different magnifications.

55.6 MPa [13]. As aluminium shears at ~45°, $\tau = \sigma_{UTS\,Al} \cdot \cos^2 45 = 27.8$ MPa. The diameter and length of the Al_3Ni fibres in the chill-cast Al–Al_3Ni eutectic were measured as ~0.8 and ~30 μm, respectively. However, this value for the diameter is probably an overestimate because of sectioning/etching effect and because of the variations within the cellular structure. A value of the smallest possible fibre diameter can be calculated from measurements of the interfibre spacing and volume fraction and a knowledge of the geometrical Al_3Ni fibre arrangement within the Al–Al_3Ni eutectic alloy. Assuming a regular hexagonal arrangement of Al_3Ni fibres, this gives $d = 0.3$ μm.

Substituting these values into Equation 12 leads to predicted values of ~143 and ~261 for the composite ultimate tensile strength, for the two extreme cases of $d = 0.8$ and 0.3 μm, respectively. The experimentally determined strength was ~219 MPa for the 800WC Al–Al_3Ni eutectic (Table I), in quite good agreement with the preceding analysis. Obviously, an exact agreement cannot be expected because of the difficulties of measuring the fibre diameter and length accurately, because Equation 12 assumes fully aligned fibres and because of the various estimates used for the other parameters in Equation 12.

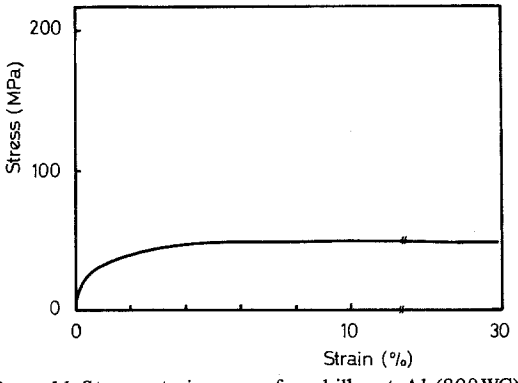

Figure 11 Stress–strain curve for chill-cast Al (800WC).

4. Conclusions

Initial solidification of the chill-cast aluminium-based eutectic alloys was slow, probably due to contact resistance of the chill–metal interface to heat transfer. Later, as the resistance of the solidifying eutectic alloy becomes large compared with chill–metal interface resistance, the solidification rate increases with the amount solidified and the distance solidified is proportional to (time)^n where n is a constant greater than 1. Experimentally, n is 1.33 ± 0.21 for the Al–Al_3Ni eutectic alloy and 1.54 ± 0.29 for the Al–Al_2Cu eutectic alloy, under the chill-casting conditions. These values of n are higher than the usual value of 0.5 and this seems to be a consequence of the variation of solid and liquid temperature gradients during solidification. This result is supported by a decrease in interfibre/lamellar spacing along the length of the solidifying ingot; i.e. from the relationship between interfibre/lamellar spacing and solidification rate ($\lambda = AR^{-1/2}$). A decreasing interfibre/lamellar spacing implies an increasing solidification rate along the length of the solidifying ingot. The observed interfibre/lamellar spacings are somewhat higher than would be predicted by the usual $\lambda = AR^{-1/2}$ relationship, probably because post-solidification coarsening can occur in the shallow thermal gradients.

Using the different chill-casting conditions results in no significant variations in the room-

temperature tensile properties of the two chill-cast aluminium-based eutectic alloys. Variations in solidification rate along the ingots for the different casting conditions are not sufficient to affect stress–strain behaviour. The room-temperature tensile properties of the chill-cast Al–Al_3Ni eutectic alloy produced using the simple chill-casting system are very similar to those obtained by Lawson and Kerr, despite the variable solidification rate along the ingot, compared to Lawson and Kerr's steady-state conditions obtained with a more complicated solidification set-up. The ultimate tensile strength is not as high as that obtained with the unidirectionally-solidified eutectic alloy prepared at a slow and constant solidification rate and the fracture strain is higher. Because of the similar deformation and fracture behaviour *within* the colonies, this suggests that the Al_3Ni fibres provide only an ineffective reinforcement in the colony walls and therefore allow considerable plastic flow in these regions. The experimentally determined ultimate tensile strength of the chill-cast Al–Al_3Ni eutectic alloy ($\sim$ 219 MPa) is in reasonable agreement with that predicted by the rule of mixtures for discontinuous fibres (between $\sim$ 142 and $\sim$ 261 MPa).

The stress–strain curves of both the present work and that of Lawson and Kerr [8] for the Al–Al_2Cu eutectic alloy show a larger work-hardening effect compared to that of Cantor *et al.* [7] for the unidirectionally-solidified alloy. As the solidification rates in the present work and that of Lawson and Kerr were greater than that used by Cantor *et al.* a greater work-hardening effect would be expected as the interlamellar spacings were smaller ($\lambda = AR^{-1/2}$) resulting in a greater volume fraction of the matrix being constrained.

The ultimate tensile strength and fracture strain values of the chill-cast Al–Al_2Cu eutectic alloy are lower than those for either the unidirectionally-solidified alloy or Lawson and Kerr's solidified Al–Al_2Cu eutectic alloy. Unlike the Al–Al_3Ni chill-cast eutectic, the stress–strain curves for the chill-cast Al–Al_2Cu eutectic show approximately 50% less plastic deformation than the stress–strain curves obtained by either Cantor *et al.* [7] or Lawson and Kerr [8] for the unidirectionally-solidified eutectic. This implies that for the chill-cast Al–Al_2Cu eutectic, there is no easy flow within the colony walls but that large coarse Al_2Cu within the colony walls leads to premature failure and a lower ultimate strength and fracture strain.

Acknowledgements

The authors would like to thank the Science Research Council for financial support during this research programme. Professor R. W. Cahn, Head of Materials Science, at Sussex University for provision of laboratory facilities and Dr R. D. Doherty for his comments during the course of the work.

References

1. F. HARGREAVES, *J. Inst. Met.* **37** (1927) 106.
2. W. WEART and D. MACH, *Trans, AIME* **212** (1968) 664.
3. L. M. HOGAN, R. W. KRAFT and F. D. LEMKEY in "Advances in Materials Research" Vol. 5, edited by H. Herman (Wiley, New York, 1971) p. 154.
4. R. W. HERTZBERG, F. D. LEMKEY and J. A. FORD, *Trans. Met. Soc. AIME* **233** (1965) 342.
5. F. D. GEORGE, J. A. FORD and M. J. SALKIND, Metal Matrix Composites Special Tech. Publ. No. 438 (American Society for Testing Metals, Philadelphia, 1968) p. 59.
6. M. SALKIND, F. D. GEORGE and B. J. BAYLES, Investigation of Matrix Strengthening Mechanisms in Al_3Ni Whisker Reinforced Aluminium Progress report Contract No. 66-0206-d, United Aircraft Research Laboratories, East Hartford, Connecticut, September 1966.
7. B. CANTOR, G. J. MAY and G. A. CHADWICK, *J. Mater. Sci.* 8 (1973) 830.
8. W. H. S. LAWSON and H. W. KERR, *Met. Trans.* **2** (1971) 2853.
9. H. S. CARSLAW and J. C. JAEGER, "Conduction of Heat in Solids", 2nd edn (Oxford University Press, London, 1959).
10. M. C. FLEMINGS, "Solidification Processing" (McGraw-Hill, New York, 1974) p. 9.
11. G. E. NEREO, R; F. POLICH and M. C. FLEMINGS, *Trans. AFS* **73** (1965) 1.
12. E. MARBURG, *Trans AIME* **197** (1957) 157, 1553.
13. F. S. J. JABCZYNSKI, D.Phil. thesis, Sussex University, 1979.
14. R. D. DOHERTY and D. A. MELFORD, *J. Iron Steel Inst.* **204** (1966) 1131.
15. J. D. LIVINGSTONE, H. E. CLINE, E. F. KOCH and R. R. RUSSELL, *Acta Met.* **18** (1970) 399.
16. H. LILHOT and A. KELLY, Proceedings of a Conference on the Relation between Properties and Microstructure, Haifa, Israel, 1969 (Israel University Press, Jerusalem, 1969).
17. A. KELLY and G. J. DAVIES, *Metall. Rev.* **10** (1965) No. 37.
18. A. KELLY and W. R. TYSON, Proceedings of the 2nd International Materials Symposium, California, 1964 (John Wiley New York and London, 1964).

Received 27 November 1980 and accepted 11 February 1981.